



Evolution of Nanostructures While Calcining of Arc Discharge Fe–C Soot

S.A. Novopashin*, M.A. Serebryakova, A.V. Zaikovskii

Katateladze Institute of Thermophysics, Novosibirsk - 630090, Russia.

ARTICLE DETAILS

Article history:

Received 31 August 2015

Accepted 07 September 2015

Available online 08 September 2015

Keywords:

Arc Discharge Soot

Iron Oxide Nanoparticles

Calcination

ABSTRACT

The present research aims of elaborating a new manufacturing technology of iron oxide nanoparticles. Composite Fe-C anode sputtering in a low-pressure arc discharge has been used to produce Fe-containing nanoparticles on a carbon matrix. The manufactured material was calcined in air up to 800 °C. This procedure resulted in the formation of iron oxides and oxidation of carbon and its conversion into gas phase. The results show the changes in morphology, chemical composition, crystalline phases, and magnetic susceptibility properties with calcination temperature.

1. Introduction

Use of the plasma-arc method for the synthesis of magnetic nanoparticles encapsulated in a carbon jacket began with the work of Kretschmer [1] on fullerene synthesis. Opening the possibility of encapsulating atoms and nanocrystals within fullerene structures [2] led to the beginning of exploration of the magnetic properties of encapsulated atoms for the example of gadolinium carbide [3]. Plasma-arc synthesis and systematic investigation of the magnetic properties of nanoparticles obtained by spraying composite graphite–transition metal electrodes are presented in [4]. The plasma-arc method uses an electric carbon DC arc with a hot cathode in an inert gas atmosphere at reduced pressure. The metal precursors are put into a cavity drilled in a graphite electrode and are then sprayed together with graphite. Under these conditions, the discharge is maintained by thermal emission of electrons from the cathode. High temperatures in the zone of arc glowing lead to thermal spraying of the anode material. A flow of high-temperature products of atomic spraying into the buffer gas medium is formed. Mixing the flowing products with the buffer gas leads to cooling, heterogeneous condensation, and chemical reactions in the spray products. As a result, metal particles which are “packed” into the carbon material are formed. The determining parameters of the synthesis process are the buffer gas pressure and type, discharge current and voltage, electrode geometry and composition, and molar content of the precursor in the sprayed electrode.

The interest in preparation and study of magnetic nanoparticles covered by an inert shell [5,6] is connected with both the possibility of preventing the coagulation and oxidation of magnetic nanoparticles and the need to ensure biocompatibility in medical applications [7,8]. When annealing magnetic nanoparticles with a carbon shell in an oxygen atmosphere, oxidation of the chemical components of the material occurs, as well as changes in the chemical composition and crystal structure of the nanoparticles. Thus, the changes in the properties of magnetite nanoparticles with a carbon shell upon annealing in air are studied in [9].

In the present study, we investigated the changes in morphology, chemical composition, and magnetic susceptibility of at annealing the iron - carbon soot synthesized by the plasma-arc method. The material was annealed in air to a temperature of 800 °C. To characterize the material, transmission electron microscopy (TEM), Raman spectroscopy (RS), thermal gravimetric analysis (TGA), X-ray analysis (XRD), and magnetometry were applied.

2. Experimental Methods

The experiments were carried out in a direct current electric arc, which had a current of 120 A, in a buffer gas (helium) at 50 Torr. The spray electrode (anode) was a graphite rod 70 mm in length and 7 mm in diameter. A hole (with a diameter of 4 mm) was drilled in the center of the electrode to be filled with graphite–iron mixture powder. The Fe/C weight ratio was 2/1. Monatomic spray products were diffused in the buffer gas from the hot zone of the arc, which resulted in cooling and heterogeneous condensation of the spray products. The composite material was precipitated on a cooled shield located 5 cm from the arc discharge area. The synthesized material consisted of iron-containing nanoparticles on a carbon matrix. In the second step, the synthesized Fe-C composite was calcined for two hours in air at 200, 300, 400, 450, 500, 550, 600, 700, and 800 °C. This procedure resulted in the formation of Fe oxides and oxidation of carbon and its removal into the gas phase. TEM, XRD, TGA, RS, and magnetic susceptibility measurements were used to test the material properties at every step.

High-resolution TEM images were obtained using a JEM-2010 electron microscope (JEOL, Japan) with lattice-fringe resolution of 0.14 nm and accelerating voltage of 200 kV. The high-resolution images of periodic structures were analyzed by the Fourier method. Local energy-dispersive X-ray analysis (EDXA) was carried out using an EDX spectrometer (EDAX Co.), which was fitted with a Si (Li) detector, at a resolution of 130 eV. The samples for the HRTEM study were prepared on a perforated carbon film mounted on a copper grid. XRD analysis was carried out using a Bruker D8 Advance diffractometer, which was equipped with a Lynxeye (1D) linear detector, over the angular range of 10–75° at $2\theta = 0.05^\circ$ with a storage time of 1 s for each point. Monochromatic CuK-radiation (1.5418 Å) was applied in these experiments. TGA experiments were performed using a DTG60 H instrument (Shimadzu Scientific Instruments). The Raman spectra were taken on a Spex Triplemate instrument (Princeton Instruments, USA) at the wavelength of 488 nm. Magnetic susceptibility was measured by an MS2 susceptibility/temperature system (Bartington, Great Britain).

3. Results and Discussion

3.1 Morphology of Material

Electron microscopy of the synthesized material indicated that it consisted of iron-containing nanoparticles of 5–10 nm (Fig. 1) embedded in amorphous carbon matrix. Calcination in air resulted in carbon removal, oxidation of iron and coagulation of nanoparticles (Fig. 2 and Fig. 3). The morphology was transformed from separate nanoparticles into 3D randomly connected structures whose size grew as the temperature of calcination increased.

*Corresponding Author

Email Address: sanov@itp.nsc.ru (S.A. Novopashin)

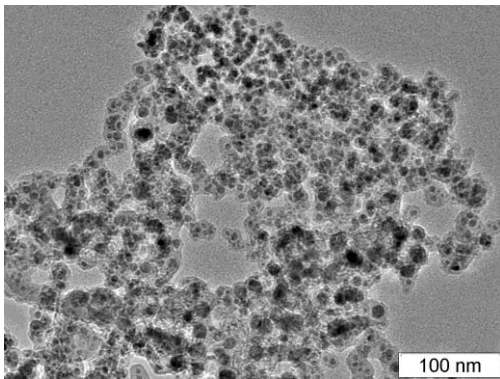


Fig. 1 The morphology of the synthesized material.

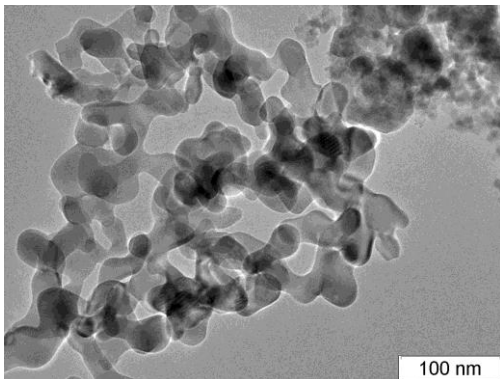


Fig. 2 The morphology of the material calcined at 400 °C.

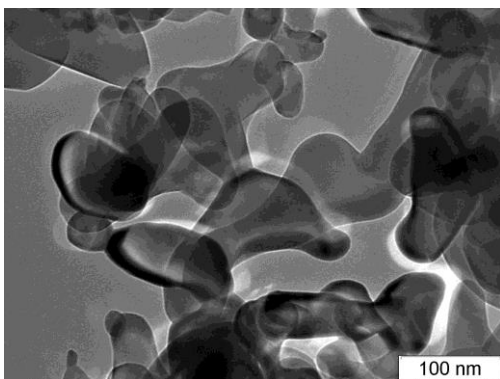


Fig. 3 The morphology of the material calcined at 800 °C.

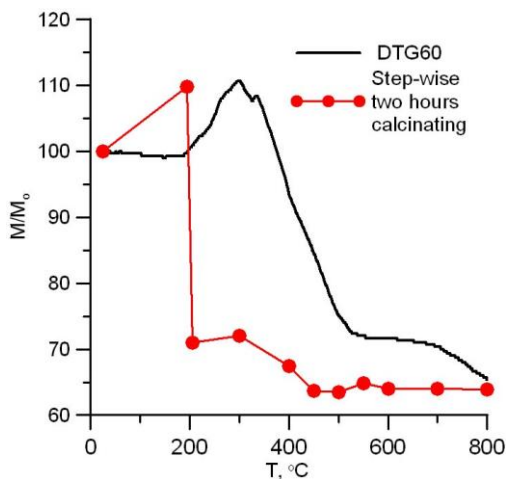


Fig. 4 Thermogravimetric analysis.

3.2 Thermogravimetric Analysis

TGA of synthesized materials was carried out in two ways: firstly by the use of a DTG60 device, and secondly by step-wise calcination at some temperatures for two hours with measurement of the weight loss. Data are presented in Fig. 4. Both curves show the weight increase at the initial stage. Obviously, it is due to oxidation of iron-containing particles. The stepwise analysis demonstrates that at 200 °C the greatest part of the carbon reacts with oxygen (Fe nanoparticles probably served as a catalyst) and is removed from the sample. The reason for the observed difference is the fact that the reaction times differed considerably between the two cases.

3.3 Phase composition

XRD spectroscopy shows that the synthesized material consists of graphite, iron, and iron carbide (Fig. 5). Calcination of this material results in a change in composition. Calcination at 300 °C resulted in the appearance of both α -Fe₂O₃ and γ -Fe₂O₃ crystalline forms of iron oxide, but iron and iron carbide lines disappeared from the spectrum (Fig. 6). Further calcination resulted in the disappearance of γ -Fe₂O₃ and growth in the intensity of α -Fe₂O₃.

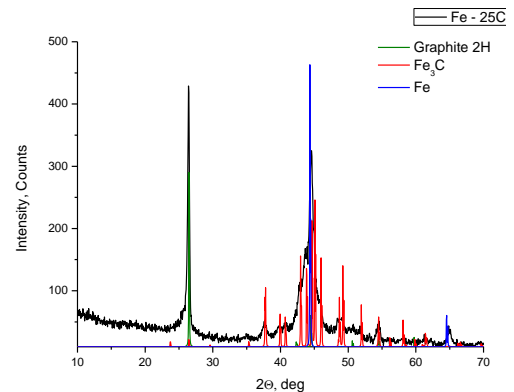


Fig. 5 XRD spectrum of synthesized material.

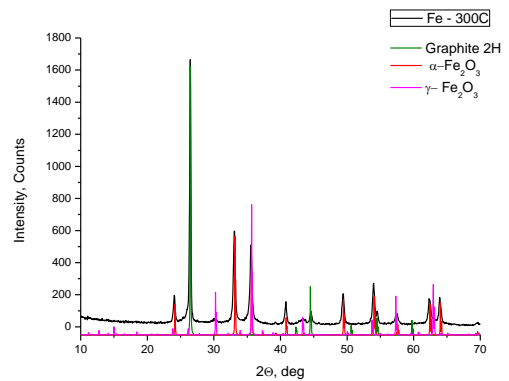


Fig. 6 The XRD spectrum of material calcined at 300 °C.

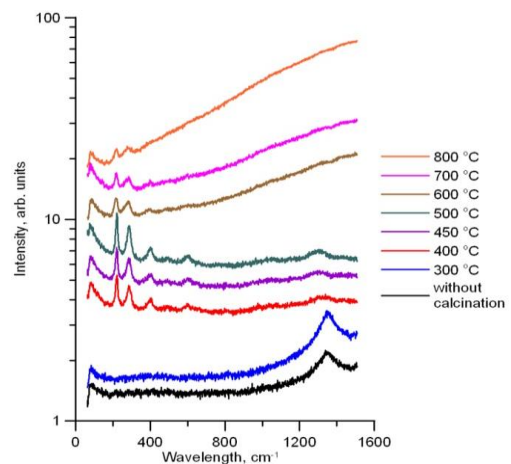


Fig. 7 Raman spectrum of material calcined at different temperatures.

3.4 Raman spectroscopy

Raman spectra of materials calcined at different temperatures are shown in Fig. 7. No line is observed for the material that was synthesized and calcined at 300 °C due to the carbon matrix. For higher calcination temperatures the observed lines are at 225, 299, 400, 500, and 613 cm^{-1} . Most lines identify $\alpha\text{-Fe}_2\text{O}_3$ and $\gamma\text{-Fe}_2\text{O}_3$. The line at 500 cm^{-1} is the sum of $\gamma\text{-Fe}_2\text{O}_3$ (strong intensity) and $\alpha\text{-Fe}_2\text{O}_3$ (weak intensity) [10]. This line disappears for calcination temperatures higher 500 °C, confirming the XRD data.

3.5 Magnetic susceptibility

Magnetic susceptibility was measured in two ways. First, the specific magnetic susceptibility of the samples obtained by stepwise calcination at different temperatures was measured at room temperature. The mass loss during calcination was taken into account in accordance with Fig. 4. Second, the magnetic susceptibility of the initial sample was measured while heating the sample and then cooling it in air. For comparison with the data of the stepwise measurements it was suggested that mass loss was linear with time during the stage of increasing temperature. The results are shown in Fig. 8. Both graphs show that the magnetic susceptibility falls for temperatures higher than 400 °C. The measurements of magnetic susceptibility while cooling showed the irreversible change of the phase state.

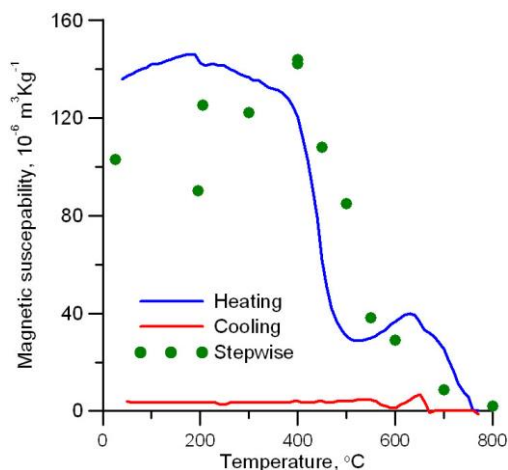


Fig. 8 Magnetic susceptibility vs. temperature.

4. Conclusion

Composite Fe-C anode sputtering in a low pressure arc discharge has been used to produce Fe-containing nanoparticles on a carbon matrix. The manufactured material was calcined in air up to 800 °C. This procedure resulted in the formation of iron oxides and oxidation of carbon and its conversion into gas phase. The results show the changes in morphology, chemical composition, crystalline phases, and magnetic susceptibility properties with calcination temperature.

The chemical composition of the synthesized material consists of graphite, iron, and iron carbide. The average size of iron-containing particles grew from 10 to 100 nm when they were calcined at a temperature of 800 °C. XRD analysis and Raman spectroscopy showed decreases in magnetic susceptibility at calcination temperatures higher than 400 °C as a result of phase transition in iron oxide from $\gamma\text{-Fe}_2\text{O}_3$ to $\alpha\text{-Fe}_2\text{O}_3$.

Acknowledgement

This research was funded by the Russian Ministry of Education and Science. Project Identifier: RFMEFI60414X0004.

References

- [1] W. Kratschmer, L.D. Lamb, K. Fostiopoulos, D.R. Hoffman, Solid C-60 – a new form of carbon, *Nature* 348 (1990) 354–358.
- [2] C.S. Yannoni, M. Haimkiss, M.S. De Vries, Scandium clusters in fullerene cages, *Science* 256 (1992) 1191–1192.
- [3] S.A. Majetich, J.O. Artman, M.E. McHenry, Preparation and properties of carbon coated magnetic nanoparticles, *Phys. Rev. B* 48 (1993) 16845–16848.
- [4] E.M. Brunsmann, R. Sutton, E. Bortz, Magnetic properties of carbon coated, ferromagnetic nanoparticles produced by carbon-arc method, *J. Appl. Phys.* 75 (1994) 5882–5884.
- [5] T. Gegechkori, G. Mamniashvili, E. Kutelia, Technology for production of magnetic carbon nanopowders doped with iron and cobalt nanoclusters, *J. Magn. Magn. Mater.* 373 (2015) 200–206.
- [6] S. Chaitoglou, M. Reza Sanaee, N. Aguiló-Aguayo, E. Bertran, Arc-discharge synthesis of iron encapsulated in carbon nanoparticles for biomedical applications, *J. Nanomater.* (2014) Article ID 178524.
- [7] H. Macková, D. Horák, G.V. Donchenko, Colloidally stable surface-modified iron oxide nanoparticles: Preparation, characterization and anti-tumor activity, *J. Magn. Magn. Mater.* 380 (2015) 125–131.
- [8] I. Sharifi, H. Shokrollahi, S. Amiri, Ferrite-based magnetic nanofluids used in hyperthermia applications, *J. Magn. Magn. Mater.* 373 (2012) 903–915.
- [9] A. Jafari, S. Farjami Shayesteh, M. Salouti, K. Boustani, Effect of annealing temperature on magnetic phase transition in Fe_3O_4 nanoparticles, *J. Magn. Magn. Mater.* 379 (2015) 305–312.
- [10] D.L.A. de Faria, S.S. Venancio, M.T. de Oliveira, Raman microspectroscopy of some iron oxides and oxyhydroxides, *J. Raman Spectrosc.* 28 (1997) 873–878.